ELSEVIER

Agricultural and Forest Meteorology 86 (1997) 107–125

AGRICULTURAL AND FOREST METEOROLOGY

Radiation regime and canopy architecture in a boreal aspen forest

J.M. Chen [a,*], P.D. Blanken [b], T.A. Black [b], M. Guilbeault [a], S. Chen [b]

[a] *Applications Division, Canada Centre for Remote Sensing, 588 Booth Street, Ottawa, Ont. K1A 0Y7, Canada*
[b] *Department of Soil Science, University of British Columbia, Vancouver, B.C. V6T 1Z4, Canada*

Received 16 September 1996; accepted 26 September 1996

Abstract

This study was part of the Boreal Ecosystem–Atmosphere Study (BOREAS). It took place in a mature aspen forest in Prince Albert National Park, Saskatchewan, Canada. The aspen trees were 21.5 m high with a 2–3 m high hazelnut understory. The objectives were: (1) to compare the radiation regime beneath the overstory before and after leaf emergence; (2) to infer the structural characteristics of the aspen canopy leaf inclination and clumping; (3) to determine the seasonal course of the leaf area index (L) for both the overstory and understory. Above-stand radiation measurements were made on a 39 m walk-up tower, and understory radiation measurements were made on a tram which moved horizontally back and forth at 0.10 m s^{-1} on a pair of steel cables 65 m in length suspended 4 m above the ground. In addition, several LI-COR LAI-2000 Plant Canopy Analyzers were used to determine the effective leaf area index and the zenith angle dependent extinction coefficient ($G(\theta)$) for both the aspen and the hazelnut throughout the growing season. These measurements were supplemented with destructive sampling of the hazelnut at the peak of the growing season. Before leaf emergence, the ratios of below- to above-aspen solar radiation (S), photosynthetic photon flux density (PPFD) and net radiation (R_n) during most of the day were 0.58, 0.55 and 0.47, respectively. By midsummer, these ratios had fallen to 0.33, 0.26 and 0.26, respectively. The aspen $G(\theta)$ was relatively invariant with θ, within ± 0.05 of 0.5 throughout the growing season, indicating a spherical distribution of leaf inclination angles (i.e. the leaves were randomly inclined). The hazelnut $G(\theta)$ has a cosine response with respect to θ, which was consistent with the generally planophile leaf distribution for hazelnut. Using canopy gap size distribution theories developed by Chen and Black (1992b, *Agric. For. Meteorol.*, 60: 249–266) and Chen and Cihlar (1995a, *Appl. Opt.*, 34: 6211–6222) based on Miller and Norman (1971, *Agron. J.*, 63: 735–738), the foliage clumping index (Ω) of the aspen canopy was derived from high-frequency tram measurements of PPFD. The aspen Ω was fairly constant with θ, but showed a small seasonal variation, with a minimum value of 0.70 in the midsummer. The hazelnut Ω was found to be 0.98 determined using the L from the destructive sampling, indicating no clumping. After corrections for clumping and the wood area index (α), the seasonal course of L near the tower for both aspen and hazelnut was determined, with maximum L of 2.4 and 3.3 for the aspen and hazelnut, respectively. © 1997 Published by Elsevier Science B.V.

Keywords: Aspen forest; Radiation regime; Canopy; *Populus tremuloides*

* Corresponding author.

PII S0168-1923(96)02402-1

1. Introduction

Aspen (*Populus tremuloides*) is one of the major deciduous species of the boreal forest, occupying approximately 20% of the southern boreal landscape (Kabzems et al., 1986). As part of BOREAS, which has the goal of understanding the contribution of boreal ecosystems to the global carbon budget and their response to global change, an intensive investigation site was selected in a horizontally extensive mature aspen stand. Measurements of diurnal fluxes of CO_2, water vapor, heat and other trace gases were made on a micrometeorological tower for nearly a complete seasonal cycle (Black et al., 1996). These measurements provide a solid foundation for understanding the functionalities of this species, but the data can only be used for other areas in the landscape when the stand characteristics governing the energy and gas exchange are fully described.

Solar radiation is the driving force for biological activities resulting in the observed energy and gas fluxes. Plant canopies interact in various ways with solar radiation depending on their canopy structure. One of the basic canopy parameters is the leaf area index (LAI) defined as one-half the total leaf area per unit ground surface area (Chen and Black, 1992a). Many ecological and climate models require LAI as an input (Sellers et al., 1986; Running and Coughlan, 1988; Bonan, 1993). Different patterns of leaf angular and spatial distributions also have important effects on the transmission and absorption of solar radiation through the canopy (Nilson, 1971). Quantification of these effects involves the complex plant canopy architecture which is often avoided in many models, especially those for large area applications. However, the architecture of plant canopies of the same type (deciduous, conifer, agricultural crops, grassland, etc.) is often similar, and it would be possible and simple to just use type-specific canopy architectural parameters. One parameter is the projection coefficient ($G(\theta)$) as a function of solar zenith angle θ, which defines the effect of the foliage angular distribution. It can be taken as 0.5 for almost all types of canopies as the first approximation. The other is the clumping index (Ω) quantifying the effect of non-random foliage spatial distribution. This parameter may be strongly type dependent. The clumping index for boreal conifer stands has been comprehensively investigated by Chen (1996a), but such data are lacking for boreal deciduous forests. The aspen stand investigated here has two distinct layers of foliage: the aspen overstory and the hazelnut understory with approximately the same LAI. This distinct canopy architecture therefore requires special attention in the radiation modeling. Measurements of radiation in deciduous forests have been performed in the past and various radiative transfer processes investigated (Miller, 1967b; Miller et al., 1976; Stoner et al., 1978). To meet the requirements of models applied to various scales, the field data acquired in this study have been analyzed at several levels of detail. The goal of this study was to extract the various canopy parameters and to demonstrate their relative importance in modeling radiation and other biophysical processes in the canopy. The specific objectives are: (1) to compare the radiation regime beneath the overstory before and after leaf emergence; (2) to infer the structural characteristics of the aspen canopy (leaf inclination and clumping); (3) to determine the seasonal courses of LAI of both the aspen overstory and hazelnut understory.

2. Theory

Assuming the azimuthal homogeneity, the probability $P(\theta)$ of a solar beam penetrating through a plant canopy with a leaf area index of L at the zenith angle of θ is generally described by (Nilson, 1971):

$$P(\theta) = e^{-G(\theta)\Omega L/\cos\theta} \tag{1}$$

When measurements of $P(\theta)$ are made at several zenith angles, the product of Ω and L can be derived without the knowledge of $G(\theta)$. This product is a unique quantity determining the radiation environment under the

canopy and is called the effective LAI, denoted by L_e (Chen et al., 1991). Chen and Black (1992b) adopted the theorem of Miller (1967a) for the calculation of L_e:

$$L_e = \int_0^{\pi/2} \kappa(\theta) \sin\theta \, d\theta \tag{2}$$

where $\kappa(\theta)$ is the mean contact number, calculated using

$$\kappa(\theta) = \cos\theta \ln[1/P(\theta)] \tag{3}$$

The calculation of L_e requires measurements of $P(\theta)$ covering the full zenith angle range from zero to $\pi/2$. The LAI-2000 Plant Canopy Analyzer (LI-COR, Lincoln, NE, USA) is therefore well suited for this purpose. However, this instrument generally overestimates $P(\theta)$ and hence underestimates L_e because of the effect of blue-light scattering in the canopy. $\kappa(\theta)$ is used in this paper to investigate this effect.

Rigorous estimation of global radiation under the canopy requires separate equations for the direct and diffuse components. However, an approximate equation similar to Eq. (1) can be used for this purpose (Black et al., 1991):

$$S_{tu} = S_t \exp(-KL_e) \tag{4}$$

where S_{tu} and S_t are the global solar irradiance beneath and above the canopy, respectively, and K is the bulk extinction coefficient defined as

$$K = G_t(\theta)/\cos\theta \tag{5}$$

$G_t(\theta)$ is defined as the projection coefficient for the combined direct and diffuse radiation. It is conceptually similar to $G(\theta)$, but their values can be considerably different. Black et al. (1991) found that $G_t(\theta)$ depends strongly on the ratio of direct to diffuse radiation above the stand because of the scattering of radiation in the canopy. Eq. (4) provides a convenient way to estimate radiation beneath the canopy, and similar equations can also be used for the photosynthetically active radiation (PAR) and net radiation, but the bulk extinction coefficients are expected to be different from that for the global radiation because of different scattering coefficients of leaves for these radiation variables and different proportion of the direct radiation in the various parts of the solar spectrum. When S_{tu} and S_t are measured, the bulk extinction coefficient for global radiation can be calculated from Eq. (4), i.e.

$$K = \frac{\ln(S_t/S_{tu})}{L_e} \tag{6}$$

To determine LAI from L_e, it is required to know Ω. If leaves are randomly distributed in space, Ω equals unity. However, for most plant canopies, leaves are grouped into tree crowns and branches, resulting in Ω smaller than unity. When leaves are clumped, not only does $P(\theta)$ increase for the same LAI, but also the probability of observing a large gap increases. A canopy gap size distribution can therefore be used to quantify Ω. Such a canopy gap size distribution can be obtained from the measurements of PAR trace using a radiation tram beneath the canopy. The theories have been fully described by Chen and Black (1992b) and Chen and Cihlar (1995a). In this paper, both theories are used. Chen and Cihlar's equation for calculating Ω (Ω_E in their paper) is

$$\Omega = \frac{[1 + F_m(0) - F_{mr}(0)]\ln[F_m(0)]}{\ln[F_{mr}(0)]} \tag{7}$$

where $F_m(0)$ is the measured total canopy gap fraction and equals $P(\theta)$, and $F_{mr}(0)$ is the gap fraction for a canopy with randomly positioned leaves having the same LAI. Whereas $F_m(0)$ can be measured as the transmittance of direct radiation at the zenith angle of interest, $F_{mr}(0)$ is obtained through processing the curve $F_m(\lambda)$, which is the accumulated gap fraction resulting from gaps larger than or equal to λ. $F_m(\lambda)$ can be

derived from the tram measurements. According to Miller and Norman (1971), the pattern of gap size accumulation for a random canopy, denoted by $F_r(\lambda)$, can be predicted from LAI and the foliage element width. By comparing $F_m(\lambda)$ with $F_r(\lambda)$, large gaps appearing at probabilities larger than the prediction of $F_r(\lambda)$ can be identified and removed from the total gap accumulation. $F_{mr}(\lambda)$ is $F_m(\lambda)$ brought to the closest agreement with $F_r(\lambda)$, representing the case of a random canopy with the same LAI. In the calculation of $F_r(\lambda)$, LAI is required, but it is unknown. Chen and Cihlar (1995a) solved the problem by using an iteration method.

The equation of Chen and Black (1992b) for calculating the clumping index is

$$\Omega = \frac{L_{e\theta}}{L_{Ep} L_{c\theta}} \tag{8}$$

where

$$L_{e\theta} = -\ln[P(\theta)] \tag{9}$$

$$L_{c\theta} = -\ln[P_c(\theta)] \tag{10}$$

and

$$L_{Ep} = \ln\left\{ \frac{(1+\alpha) L_{c\theta} \exp(-L_{c\theta})}{\sqrt{2(1+\alpha)\exp[-(L_{e\theta}+L_{c\theta})] - (1+2\alpha)\exp(-2L_{c\theta})} - \exp(-L_{c\theta})} \right\} \tag{11}$$

In the above equations, $P(\theta)$ is the gap fraction at the solar zenith angle θ, $P_c(\theta)$ is the imaginary canopy gap fraction when all foliage clumps are opaque, L_{Ep} is calculated from the intermediate variables $L_{e\theta}$ and $L_{c\theta}$, and α is a small value compensating the truncated higher-order Poisson terms, being $L_{c\theta}\exp(-L_{Ep})/3$. In the calculation of L_{Ep}, α is first taken to be zero to obtain a precursory L_{Ep} from Eq. (11), which is then used to determine α. The above equations show that to obtain Ω, only two parameters need to be obtained from measurements: $L_{e\theta}$ and $L_{c\theta}$. As $P(\theta)$ for calculating $L_{e\theta}$ is readily available from radiation transmittance, the only thing missing for calculating Ω is $P_c(\theta)$ or $L_{c\theta}$. Chen and Black (1992b) found that $L_{c\theta}$ can be derived from a measured canopy gap size distribution curve under the assumption of random spatial distribution of foliage clumps (see examples in Section 4). Chen and Cihlar (1995b) found that this assumption, though reasonable, often caused negative biases in the Ω estimation. Chen and Cihlar's method avoids this assumption, and therefore is generally more accurate. The calculation of LAI in this paper is based on Chen and Cihlar's method, and Chen and Black's method is used for comparison.

3. Site description and experimental procedure

The study was conducted in a southern boreal aspen stand located in Prince Albert National Park, Saskatchewan, Canada (53.629°N, 106.20°W). The aspen forest was an even-aged 70-year-old mature stand with a low stem density of 828 trees ha^{-1}. Mean canopy height was 21.5 m with an average diameter at breast height (DBH) of 0.199 m (SD 0.045 m). Leaves and branches were confined to the relatively narrow upper 7 m of the canopy, with the remaining trunk space bare. The extensive understory was composed mainly of hazelnut (*Corylus cornuta*) reaching an average height of 2 m. Leaves were not confined to the top of the hazelnut, but rather gradually diminished closer to the ground. By mid-summer, the hazelnut foliage was very thick and dense. A LAI-2000 Plant Canopy Analyzer was used determine the course of LAI development and $G(\theta)$. To determine the characteristics of a layer of vegetation, the LAI-2000 requires measurements to be taken both above and below the layer in question. For the aspen overstory, above-canopy readings were taken at a height of 25 m above the ground from a walk-up tower located at the study site. This was immediately followed by readings at a height of 3 m above the ground taken at two predetermined locations. Following the below-canopy

readings taken for the aspen canopy, above-canopy readings were again taken to ensure that sky conditions did not change during the time taken to make the measurements. LAI-2000 measurements of the hazelnut were taken at the same six locations used for the below-canopy aspen readings. Two of these locations were located near the base of the walk-up tower, and the remaining four were located every 25 m along a 100 m east–west transect within the footprint of the walk-up tower. Above-hazelnut readings were made by holding the LAI-2000 optical sensor well clear of the hazelnut canopy top, immediately followed by a below-canopy reading taken at the ground surface. A pair of above and below readings were taken at each of the six locations. As the LAI-2000 requires diffuse light to give reliable measurements, the instrument was used only under uniform overcast conditions, or before sunrise and after sunset. To avoid contamination of the measurements by the operator or the walk-up tower, a 180° view restrictor was used. As the LAI-2000 cannot distinguish between wood, branches and leaves, measurements taken are L_e, which must be corrected for the wood area index (α) and Ω. LAI-2000 measurements of both the aspen and hazelnut canopies were taken before leaf emergence and at several times throughout the growing season until late autumn.

Three times during the growing season, corresponding to three intensive field campaigns, three units of LAI-2000 were used at a 10 m interval along three 300 m transects extending in the southwest direction from the tower. One unit was used to acquire the above-stand reference readings every 15 s in an unattended mode at the top of the tower, and the other two were used for measurements above and below the hazelnut understory along the transects. A comparison between the transect measurements and the measurements around the tower described above was made for the purpose of converting the frequent measurements around the tower to the whole stand. We believe the transect measurements in the prevailing upwind direction are more representative of the whole stand.

Destructive measurements of the hazelnut LAI were made on 6 August, when the LAI was at its maximum. Leaves harvested in three 3 m × 3 m plots were immediately weighed on site, and 200 g of fresh leaves were randomly sampled. The L of this random sample was determined with a plant area meter (LI-3100, LI-COR) and the weight of the random sample was determined to an accuracy of 0.001 g using a 500 g balance (Mettler, Princeton, NJ, USA). The LAI of each plot was then calculated from the relationship between the random sample weight and leaf area.

Diurnal spatially averaged measurements of the radiation regime beneath the aspen overstory and above the hazelnut understory were made using a tram that moved horizontally back and forth at 0.10 m s^{-1} on a pair of steel cables oriented 338°N, 65 m in length, suspended 4 m above the ground surface. The steel cables were periodically tightened to ensure the tram maintained horizontality along the 65 m path. When the tram reached the end of the cables, a magnet made contact with a normally open switch. This sent a signal to an electronic circuitry which reversed the direction of a 0.25 hp DC motor, which pulled the tram via a fine-steel cable. The tram carried a Swissteco S-1 net radiometer and S-14 miniature net radiometer (Swissteco, Oberriet, Switzerland) to measure net radiation (R_n), shaded and unshaded Kipp and Zonen CM-5 pyranometers (Kipp and Zonen, Delft, Netherlands) to measure total solar radiation (S), where $S = S_b$(direct) + S_d(diffuse), and diffuse solar radiation (S_d), respectively, and upward- and downward-facing LI-COR 190-SB quantum sensors to measure the incident and reflected photosynthetic photon flux density (PPFD), respectively. Voltage signals from these instruments were collected with a CR10 datalogger (Campbell Scientific, Logan, UT, USA) at a scan rate of 1 Hz, with the exception of the upward-facing quantum sensor, which was scanned at a rate of 10 Hz.

4. Results

4.1. Radiation transmission characteristics

Fig. 1 shows seasonal variations in the midday PPFD values (half-hourly means) above and below the aspen overstory from early January to middle September. The above-overstory measurements were made using a

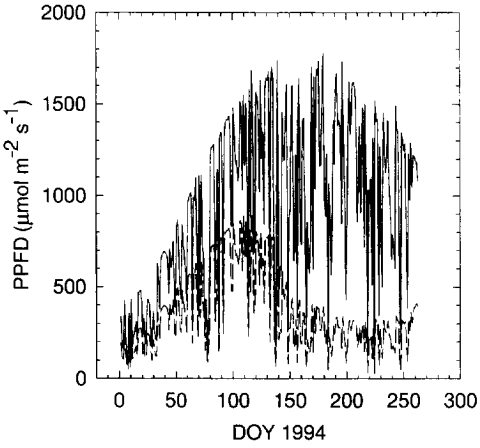

Fig. 1. Midday PPFD values above and below the aspen canopy from early January to mid-September (DOY, day of the year).

stationary sensor at 38 m, and the below-overstory measurements were made at 4 m by the tram in a round trip near solar noon. As the tram was only operated for several days at the beginning, middle and end of the growing season, many below-overstory values were calculated using the above-overstory measurements and an extinction coefficient which was characteristic of the period based on the tram data. From the below-canopy variation, it can be seen that leaf emergence began at about DOY (day of year) 110 (late April) and senescence at about DOY 260 (middle September). The attenuation of PPFD was considerable before leaf emergence because of the interception by branches and tree trunks.

Fig. 2 shows typical clear-sky pre-leaf emergence diurnal courses of above-aspen and below-aspen S (Fig. 2(a)), PPFD (Fig. 2(b)) and R_n (Fig. 2(c)) and their corresponding ratios. All ratios are large and relatively constant throughout the day, with values (SD in parentheses) of 0.58 (0.06), 0.55 (0.09) and 0.47 (0.06) for S, PPFD and R_n, respectively. This indicates that the solar zenith angle has only a small effect on the radiation transmission. It appears that the reduction in S_b transmission that occurs as the path length increases with increasing solar zenith angle is offset by an increase in S_d fraction in the total transmitted radiation. By comparison, Fig. 3 shows typical clear-sky post-leaf emergence diurnal courses of above-aspen and below-aspen S_t (Fig. 3(a)), PPFD (Fig. 3(b)) and R_n (Fig. 3(c)) and their corresponding ratios. All ratios are much smaller

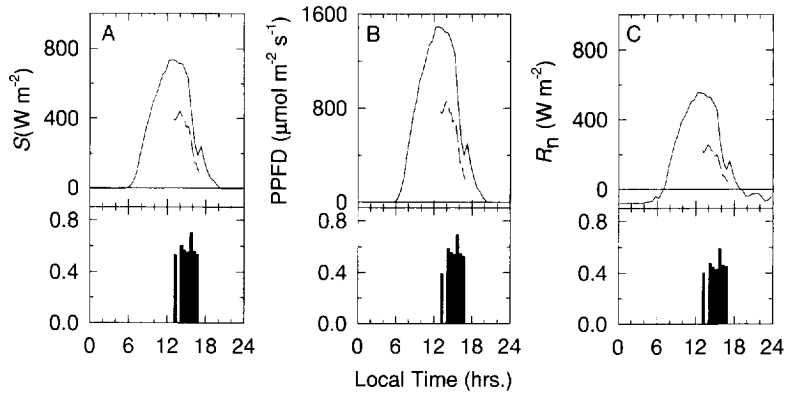

Fig. 2. Clear-sky pre-leaf emergence diurnal courses of above aspen (continuous lines) and below aspen (dashed lines) solar radiation (A), PPFD (B) and net radiation (C) as measured on 17 April 1994. Lower panels show the ratios of below to above fluxes.

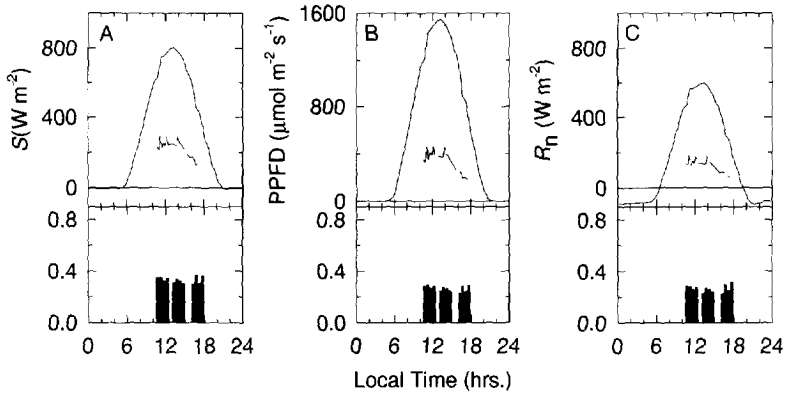

Fig. 3. Clear-sky post-leaf emergence diurnal courses of aspen (continuous lines) and below aspen (dashed lines) solar radiation (A), PPFD (B) and net radiation (C) as measured on 4 August 1994. Lower panels show the ratios of below to above fluxes.

than their pre-leaf emergence counterparts, with values of 0.33 (0.02), 0.26 (0.02) and 0.26 (0.03) for S, PPFD and R_n, respectively. Again, ratios are relatively constant and do not decrease with increasing solar zenith angles, indicating the similar effect of S_d.

A summary of the typical clear-sky pre- and post-leaf emergence ratios of below-to-above radiation measurements are shown in Fig. 4. Despite the sparse aspen canopy, post-leaf emergence ratios for all three streams of radiation are significantly lower than pre-leaf emergence ratios. Furthermore, the absence of any effect of decreasing S_b owing to increasing path length with increasing solar zenith angle is shown by the small standard deviations. The larger pre-leaf emergence standard deviations indicate that the leafed canopy is more homogeneous than the unleafed canopy. The pre- and post-leaf emergence bulk extinction coefficient (K) for the S_t, PPFD and R_n radiation streams for our forest and two other deciduous forests shown in Fig. 5 illustrates a somewhat counter-intuitive result. On a unit plant-area basis, a lower post-emergence K indicates that radiation has an easy time penetrating through a layer of the overstory canopy compared with the case when the canopy is leafless. Although there is less radiation reaching the understory when the aspen canopy is mature, the radiation that does reach the understory does so more efficiently. This is again due to the increased fraction of S_d, which decreases much less than S_b with the depth into the canopy. Multiple scattering of radiation inside the canopy is responsible for the small decrease in S_d (Ross, 1981). This result has also been found by Baldocchi et

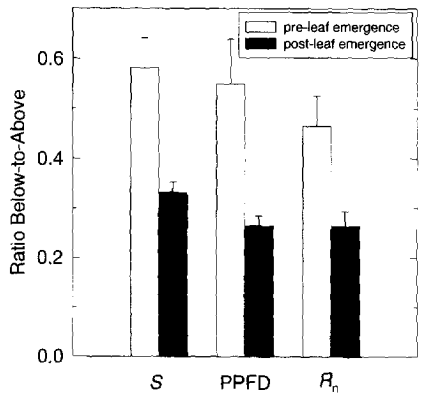

Fig. 4. Average ratios of below to above radiation measurements (+ 1 SD) before leaf emergence (17 April 1994) and after leaf emergence (4 August 1994).

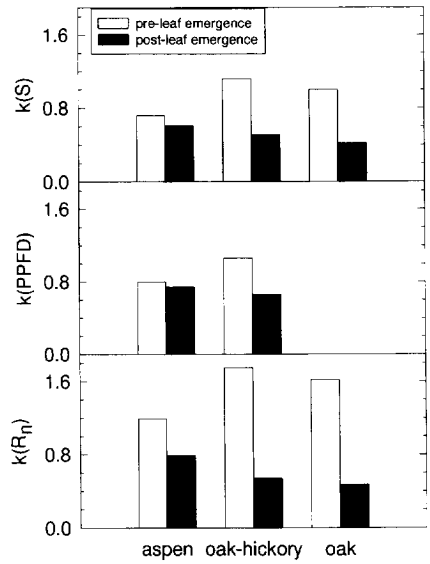

Fig. 5. Bulk extinction coefficients on a plant area basis before leaf emergence (17 April 1994) and after leaf emergence (4 August 1994) for an aspen (this study), oak–hickory (Baldocchi et al., 1984) and oak (Rauner, 1976) forest.

al. (1984) in an oak–hickory forest in central Tennessee, and in an oak forest in the Moscow region of Russia by Rauner (1976). Seasonal variation in solar zenith angle also contributes to the difference. The canopy is leafless during the time of the year when the solar zenith angle is large, thus the path length is long, especially in an erectophile canopy mainly composed of tree trunks. In contrast, a full leafed canopy occurs near the summer solstice when the solar zenith angles are small and the corresponding path lengths are short. This seasonal variation in the solar zenith angle partly explains why the Baldocchi et al. (1984) and Rauner (1976) studies found a larger contrast in K, as their pre- and post-leaf measurements were taken further apart in the year, thus maximizing the zenith angle effect. Our measurements were taken roughly equidistant from the summer solstice, thereby decreasing the zenith angle effect.

The seasonal and solar zenith angle dependence of $G(\theta)$ for the aspen (Fig. 6(a)) and the hazelnut (Fig. 6(b)) show contrasting results. For the aspen, the absence of any significant change in $G(\theta)$ ($G(\theta) = 0.5$) implies a

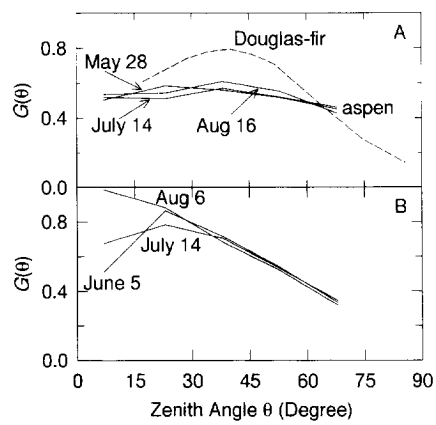

Fig. 6. Seasonal and solar zenith angle dependence of the aspen (A) and hazelnut (B) extinction coefficient. For comparison, a planophile Douglas-fir forest extinction coefficient (Black et al., 1991) is also shown.

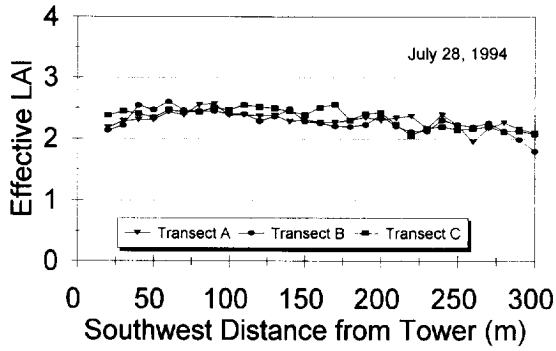

Fig. 7. Effective LAI measured by LAI-2000 along three 300 m parallel transects starting from the flux tower toward the southwest direction.

spherical or random leaf angle distribution. This is in contrast to a Douglas-fir canopy, where the $G(\theta)$ is characteristic of a planophile canopy (Black et al., 1991). Moreover, this spherical leaf distribution does not change as the aspen leaves age, as indicated by the overlapping $G(\theta)$ distributions acquired in different periods in the growing season. For the hazelnut canopy, $G(\theta)$ is characteristic of a planophile canopy structure, as the maximum extinction coefficient occurs close to the zenith and quickly falls afterwards. The understory leaves are mostly horizontal to make better use of the maximum sunlight which penetrates the canopy near solar noon. The hazelnut $G(\theta)$ shows some seasonal variation, indicating the increase in horizontal leaf area as the season progresses.

4.2. LAI and canopy architecture

Fig. 7 shows the L_e measured using the LAI-2000 along the three parallel transects extending 300 m from the flux tower in the southwest direction. Compared with conifer stands (Chen, 1996a), the variation in L_e along the

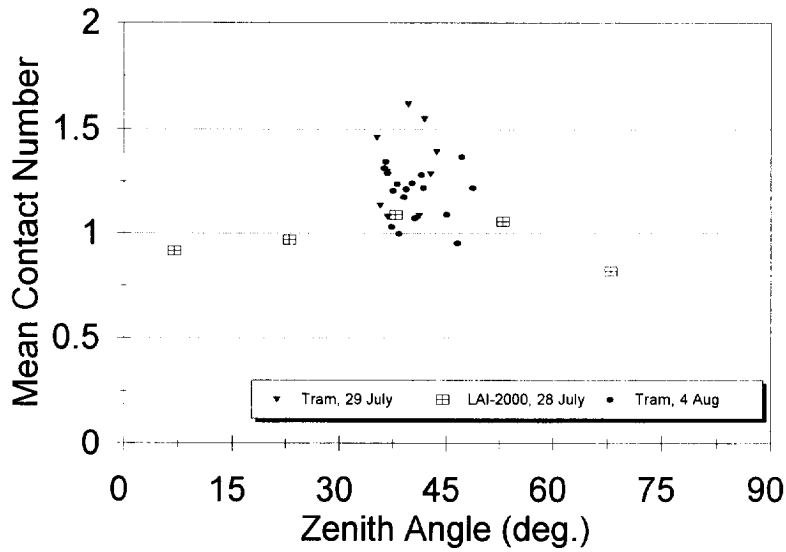

Fig. 8. Comparison of the mean contact number ($\kappa(\theta)$) measured by the LAI-2000 and the tram. From the difference, a correction factor of 1.15 is obtained for the effect of blue-light scattering on LAI-2000 measurements.

transects is very small, indicating the homogeneity of the stand at small scales, but in the first 60 m there seems to be a decreasing trend in L_e towards the tower. Based on the comparison of the mean contact number obtained from the LAI-2000 with that from the tram data (Fig. 8), the original data from the LAI-2000 have been increased by 15% to correct for the blue-light scattering effect. In Fig. 8, the LAI-2000 data are the means of 10 measurements along the tramway. Owing to spatial heterogeneity, the mean L_e value over the tramway is 20% smaller than that over the 300 m transects. The 15% correction is obtained from the relative difference between the mean of the tram data points and the mean of the LAI-2000 data in the angle range from 38° to 53°. As L_e is approximately proportional to the mean contact number (Eq. (2)), the difference in $\kappa(\theta)$ is then taken as the difference in L_e. This simple estimate may be biased because the tram data are confined to a small angle range and the scattering effect is not uniform with zenith angle: it increases with increasing zenith angle, as is evident in the small LAI-2000 value at $\theta = 68°$. As larger weights are given to $\kappa(\theta)$ at larger θ values in the L_e calculation, it is expected that the actual scattering effect is slightly larger than 15%. Based on a similar approach, Chen (1996b) found that the correction factor for the LAI-2000 ranges from 8 to 19% for conifer stands, for similar data obtained from an optical instrument named TRAC (Tracing Radiation and Architecture of Canopies). The scattering coefficients of conifer leaves are generally smaller than those of deciduous leaves, but the slight erectophile canopy structure of jack pine stands, which causes faster decrease in the gap fraction with zenith angle than the random case, may have compensated for the difference in the scattering coefficients, making the correction factor comparable. These corrections are larger than the estimates by Chen et al. (1991) based on the diffuse radiation model of Norman (1979), and should be drawn to the attention of LAI-2000 users.

The mean contact number in Fig. 8 is calculated using Eq. (3). The gap fraction $P(\theta)$ is taken as the ratio between the corresponding below- and above-canopy measurements by the LAI-2000. For the tram data, the following equation is used:

$$P(\theta) = \frac{R_{mean}(\theta) - R_{min}(\theta)}{R_{max}(\theta) - R_{min}(\theta)} \tag{12}$$

where $R_{mean}(\theta)$, $R_{min}(\theta)$ and $R_{max}(\theta)$ are the mean, minimum and maximum PPFD in the time series of a complete one-way tram run (see Fig. 9 for an example). $R_{min}(\theta)$ therefore represents the diffuse PPFD under the canopy, and R_{max} is the sum of the direct PPFD above the stand and the diffuse PPFD beneath the stand. The difference between $R_{max}(\theta)$ and $R_{min}(\theta)$ is then the direct PPFD above the stand. Such calculation is valid only if there is at least one location along the tramway at which the radiometer is fully exposed to the Sun. To

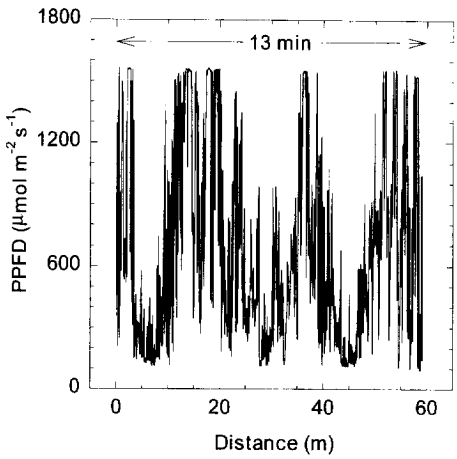

Fig. 9. Below aspen PPFD sampled at a frequency of 10 Hz on the tram system at solar noon, 1 June 1994.

ensure that this condition was met, we restrict the tram data to $\theta < 50°$. The difference between $R_{mean}(\theta)$ and $R_{min}(\theta)$ is the direct PPFD transmitted through the canopy. In using Eq. (12), we assume that $R_{min}(\theta)$ is constant along the transect. A small error is introduced under this assumption because of the spatial variability of the diffuse irradiance. It increases under large gaps and decreases under tree crowns as a result of the variation in sky light transmission and beam enrichment owing to leaf scattering. The beam enrichment can increase the diffuse irradiance by as much as 50% (Hutchinson and Matt, 1976). However, the enrichment of diffuse radiation is expected to be spatially uniform owing to the height of the canopy. In short canopies, Chen (1996) showed significant variation in $R_{min}(\theta)$ using TRAC and improved the $P(\theta)$ calculation using variable $R_{min}(\theta)$ values. The scatter of the tram data points is considerable because of the stand heterogeneity and the non-ideal tram moving direction: the tramway was oriented south–north and often traversed though long tree shadows or sunflecks around noon. The ideal tramway direction would be east–west, but other site arrangements prevented us from using this ideal orientation. However, the standard deviation of the data points is only 0.161, and the standard error of the mean (1.24) with 26 data points is 0.032, or 2.5% in 1.24.

A critical parameter used to describe canopy structure is Ω, which defines the extent by which leaves are clustered. It is also required to determine the true LAI from L_e as obtained from instruments such as the LAI-2000, which cannot distinguish the spatial distribution pattern of individual leaves. For the aspen canopy, high-frequency sampling of the PPFD during sunny conditions (Fig. 9) gives a sample of the sunfleck distribution beneath the aspen canopy. Two extremes are found in the distribution: light is either passed unaffected through the aspen canopy (maximum PPFD values in the graph) or blocked completely by canopy foliage (minimum PPFD values). The minimum is larger than zero, signifying the level of diffuse PPFD beneath the canopy. This results from both the transmission of diffuse PPFD from the sky and multiple scattering within the canopy. Values of PPFD intermediate between the maximum and minimum PPFD are due to penumbral effects. From each sunfleck (a peak, either small or large), a canopy gap is calculated after consideration of the penumbral effects (Chen and Black, 1992b). Following the approach of Chen and Cihlar (1995a), an increase in PPFD from the baseline or a reversal of a decreasing trend is taken as the beginning of a sunfleck, and the end of a sunfleck is found when either the PPFD reaches the baseline or the reversal of the decreasing trend is detected. A canopy gap size distribution is therefore determined from each 60 m tram run (the total tramway is 60 m, but the first 5 m close to the south tower was excluded to avoid tower interference). The effect of leaf fluttering owing to winds on sunfleck determination is estimated to be negligible. The quantum sensors have a very small time constant (10 μs) and respond to the light level practically instantaneously. The measurements can therefore be considered as a snapshot of the canopy, and changes in leaf positions owing to the wind along the long transect would be statistically averaged out in the final gap size distribution.

Fig. 10(a)–(c) show examples of the canopy gap size accumulation on three dates during the growing season. Fig. 10(a) is an example measured near noon on 1 June (near full leaf emergence). From the measured F_m curve, the largest gap in the tram run is identified to be close to 0.62 m and the second largest to be slightly larger than 0.38 m. The accumulated curve gradually climbs upward as the gap size decreases because of the contribution of many smaller gaps. The accumulation ends at the gap size of zero, where the accumulated gap fraction becomes the total gap fraction at the solar zenith angle. The LAI-2000 measures the total gap fraction thus representing one point on the graph. Compared with the curve F_r for the case when the canopy is random with respect to the spatial position of leaves, the probabilities for the observed large gaps are too high. In fact, if the canopy were random, the probability of observing gaps larger than 0.2 is almost zero. Many large gaps observed along the tramway resulted from tree crown and branch architecture. The large gaps appeared predominantly between tree crowns. The canopy is numerically reconstructed to approach the random condition by removing the contribution of these large gaps from the total gap fraction accumulation. This is done iteratively by removing or truncating gaps which appear at probabilities in excess of F_r. The F_r curve is modified in each iteration according to the total gap fraction after the removal of each gap. When the iteration is completed, the curve F_m is shifted downward to become F_{mr}, and the total gap fraction is reduced from 0.261 to 0.178. According to Eq. (7) the clumping index Ω is 0.84. Fig. 10(b) is another example, obtained in the

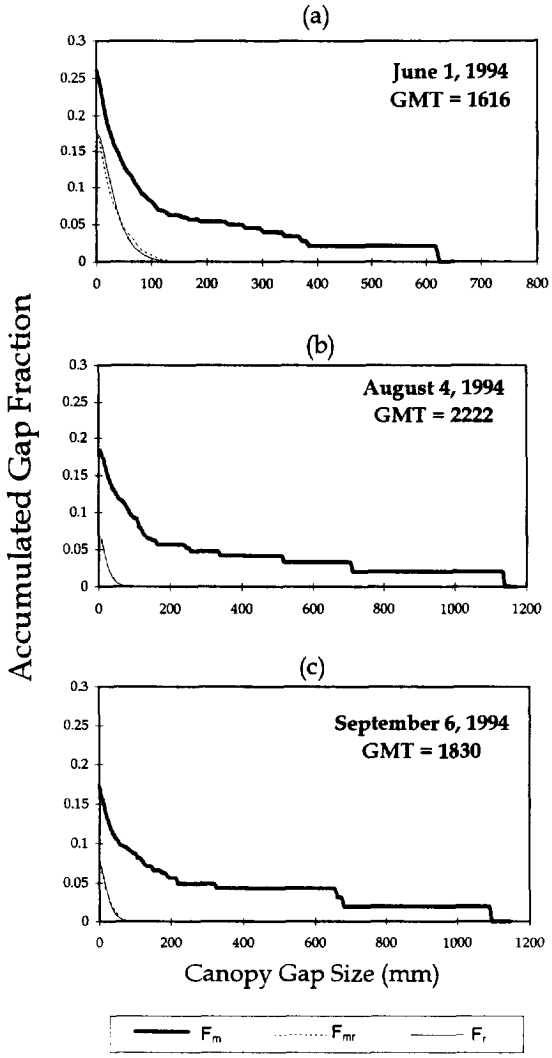

Fig. 10. Gap fraction accumulation from large to small gaps for three selected cases, where F_m is the measured accumulation curve, F_r is the case when the spatial distribution of leaves is random, and F_{mr} is F_m brought to the closest agreement with F_r through a large gap removal process. The difference between F_m and F_{mr} at the ordinate determines the clumping index.

afternoon of 4 August (midsummer). The observed total gap fraction in this case is 0.193, smaller than the case in Fig. 10(a) because of the larger solar zenith angle. The largest three gaps observed are about 1.12, 0.70 and 0.49 m. After the gap removal procedure, the curve F_{mr} overlaps closely with F_r, and the gap fraction is reduced to 0.071, resulting in $\Omega = 0.70$. In Fig. 10(c), for the case shortly before the senescence, the gap accumulation curve is similar. With the reduction of gap fraction from 0.172 to 0.078 after the gap removal procedure, $\Omega = 0.75$ is obtained.

Fig. 11(a)–(c) show the corresponding gap size distributions using the same data as in Fig. 10(a)–(c). $P(l)$ is the probability of a probe of length l falling completed within a sunfleck. If the canopy is random, ln $P(l)$ vs. l would be a straight line, with the slope inversely proportional to the size of the randomly distributed objects. The measured curves plotted in the same way are not linear, indicating that the canopy is not random. However,

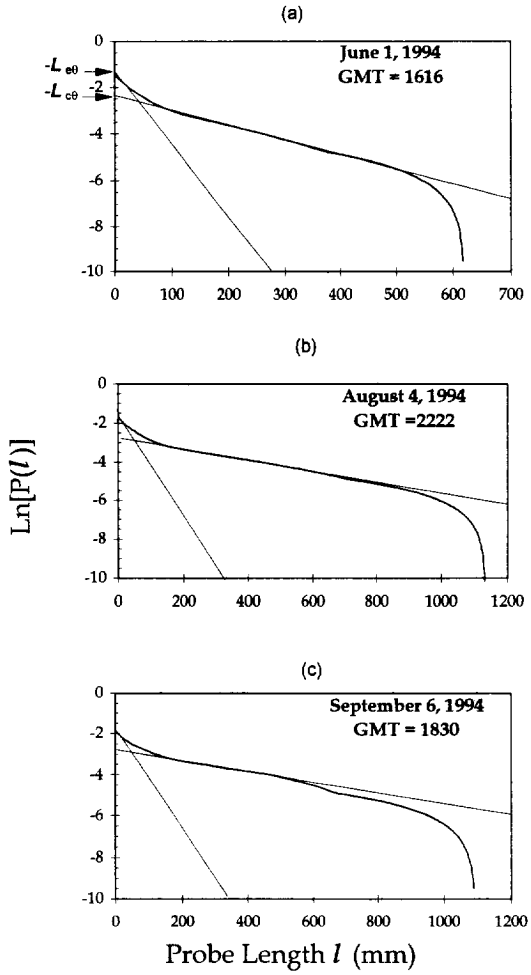

Fig. 11. Gap size distribution curves corresponding to the three cases in Fig. 10. The difference at the ordinate between the measured curve and the extrapolated line determines the clumping index, and the slopes of the extrapolated line and the tangent at $l = 0$ determine the foliage clump size and the characteristic foliage element size, respectively.

there always appears a straight portion in the middle of the curve, suggesting some randomness of the canopy. From the slope of these lines, the size of foliage clumps responsible for the apparent randomness determined using Chen and Black's (Chen and Black, 1992b) method are 0.52 m, 1.01 m and 0.84 m for Fig. 11(a)–(c), respectively. These sizes are smaller than the average size of the tree crowns, estimated to be 2–3 m, suggesting that both tree crown and branch structures are responsible for the observed gap size distribution. If the clumps are opaque, the linear trend would extend all the way to $l = 0$. However, the crowns and branches contain gaps, making ln $P(l)$ elevated from the extrapolated straight line at small l values. From a measured ln $P(l)$ vs. l curve, another straight line can be drawn as the tangent of the curve at $l = 0$. This line represents the distribution if all leaves are randomly distributed in space. In theory, the slope of this line should be related to the size of leaves. This size was found from the slope to be 47 mm, 126 mm and 120 mm for Fig. 11(a)–(c), respectively. These values are considerably larger than the average leaf characteristic width of about 35 mm. Similarly, Chen and Black (1992) and Chen and Cihlar (1995b) found that the size of foliage elements determined in the same way is always larger than the foliage elements (shoots) for conifer stands. These

consistent findings suggest that small canopy gaps are not accurately resolved, owing to the penumbral effect. There may be two reasons for the discrepancy being larger in the present study. First, the canopy is much taller than the previous cases, and therefore the penumbral effect makes it more difficult to determine small gaps. Second, aspen leaves are also grouped into twigs of 8–10 leaves. The small gaps between leaves in a group may be lost at large distances because of the penumbral effect. This means that some uncertainty exists in the calculation for Ω given above. The drop-off of the measured curve at large l values is ignored in the analysis. The theory predicts very small $P(l)$ at large l values, but, in practice, the measured largest gap is always finite, and a drop-off is inevitable.

For the calculation of Ω, only two parameters, $L_{e\theta}$ and $L_{c\theta}$, need to be determined from the sunfleck size distribution ln $P(l)$. These two parameters are first used to calculate the leaf area per unit projected clump area L_{Ep} using Eq. (11) and then used with L_{Ep} in Eq. (8) for calculating Ω. In Fig. 11(a) $L_{e\theta}$ and $L_{c\theta}$ are found to be 1.34 and 2.55, respectively. As Fig. 10(a) and Fig. 11(a) share the same data (e.g. $F_m(0) = P(\theta)$), the value of $L_{e\theta}$ equals $-\ln F_m(0)$ or $-\ln(0.261) = 1.34$. The calculated Ω in this case is 0.75. Similarly, $L_{e\theta}$ and $L_{c\theta}$ are determined to be 1.65 and 2.82 in Fig. 11(b), and 1.76 and 2.87 in Fig. 11(c). Correspondingly, the

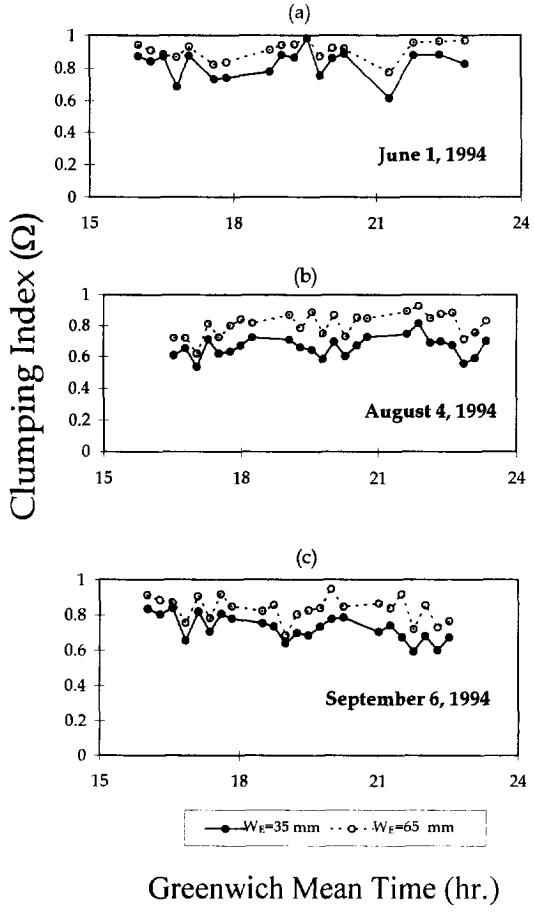

Fig. 12. The clumping index Ω measured on 3 days calculated for two characteristic leaf widths (W_E), showing little diurnal variation. From leaf samples, it is found that $W_E = 50$ mm.

calculated Ω equals 0.65 and 0.69, respectively. These three Ω values, 0.75, 0.65 and 0.69, are smaller than the corresponding values of 0.84, 0.70 and 0.75 determined from Fig. 10(a)–(c). Similar differences were reported by Chen and Cihlar (1995b) for conifer stands. These differences may be due to the assumptions made in the approach using the ln $P(l)$ distribution. The basic assumptions are: (1) foliage elements (leaves in the case of a broadleaf canopy) are randomly distributed within foliage clumps (tree crowns and branches); (2) foliage clumps are randomly distributed in space. Both assumptions have not yet been substantiated with experimental data. Tree crowns are approximately at the same height, and the natural repulsion effect in the competition for light makes it impossible to have one tree crown appear underneath the other or to have the crowns merge in depth. However, the Poisson theory used for describing the clump location allows considerable probabilities of these cases, and hence overpredicts the clumping effect (smaller Ω). Therefore, the Ω value determined using the P approach may be negatively biased. In the F approach, no such assumptions are necessary, and the Ω values are believed to be more accurate. We therefore use only the values from the F approach for further analysis. We caution, however, that both approaches suffer from the same error in determining the small gaps, owing to the penumbral effect. The error may be larger than in the previous cases (Chen and Black, 1992b; Chen and Cihlar, 1995b) because of the height of the canopy. This error is estimated to be less than 5% in the F approach, because accurate determination of the contribution of the small gaps to the total gap fraction would add about equal amounts to both $F_m(0)$ and $F_{mr}(0)$, and much of the effect is canceled in the calculation of Ω. The gap removal procedure is less affected by the detailed distribution of $F_m(\lambda)$ near $\lambda = 0$ than by the width of the curve at $\lambda < 200$ mm. This may be another advantage of the F approach. In the P approach, the value of $L_{c\theta}$ determined from ln $P(l)$ at large l values is fixed and unaffected by the missing small gaps, but the $L_{e\theta}$ is affected. When $L_{e\theta}$ is too small owing to missing the small gaps, the resulting Ω value would also be too small. This may be another reason for the smaller Ω from the P approach than from the F approach.

Fig. 12(a)–(c) show three examples of diurnal variation of Ω determined using the F approach. The calculations are made at two input values of the characteristic width of the aspen leaves, 35 mm and 65 mm. The value of 100 mm is obviously too large, but is used here for the illustration of the importance of this parameter. In all these three figures there is no consistent diurnal variation, (i.e. it does not change significantly with solar zenith angle). Chen (1996a) found significant change in Ω with solar zenith angle for conifer stands. He provided two possible reasons for the variation: (1) the disintegration of the long and thin conifer tree crowns into subcomponents such as branches as the solar zenith angle increases; (2) the possible penumbral effect which increases with solar zenith angle. As the second effect should exist in both cases, the results from the present study suggest that the first may be the cause of the variation of Ω with solar zenith angle found by Chen (1996a). Because of the small dependence of Ω on the solar zenith angle or time of the day in this case, no weighting scheme (such as that of Chen (1996a)) was used for calculating the daily mean values of Ω.

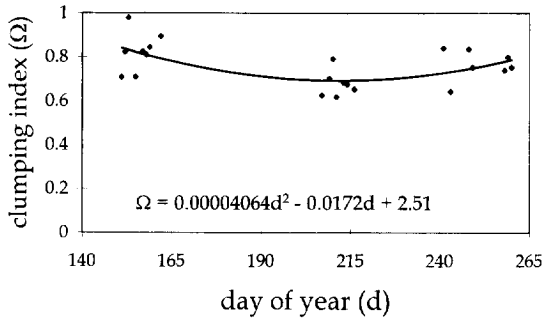

Fig. 13. The seasonal variation in Ω, showing the smallest values in the midsummer.

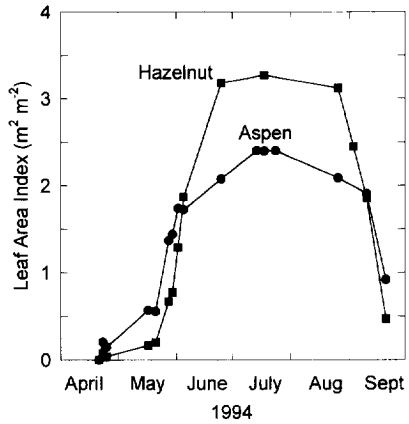

Fig. 14. Seasonal course of LAI in the vicinity of the tower for the aspen overstory and hazelnut understory. Values have been corrected for clumping, wood area index and blue-light scattering (see text).

Fig. 13 shows all the daily mean Ω values. There are three distinct groups of data corresponding to the intensive field campaigns (IFC-1, IFC-2 and IFC-3). The first group was obtained from tram runs shortly after leaf emergence. At that time, the leaves had not fully grown and therefore were less clumped (larger clumping index) than in the mid-summer case (the second group). In the autumn, starting from late August, leaf drop owing to senescence reduced LAI, and the clumping index increased slightly. A second-order polynomial curve was fitted to the data, and the seasonal variation in Ω is about 0.1. Though small, this variation is important and should be taken into account in the calculation of the seasonal variation in LAI. Chen (1996a) found that the clumping of foliage at scales larger than the shoots varied very little throughout the growing season for conifer stands because new needles grow on top of old needles and do not change much of the gap fraction and gap size distribution. However, in the aspen stand investigated here, the small gaps within tree crowns can vary significantly with leaf emergence, expansion and senescence, resulting in the observed variation in the clumping index.

The clumping index of the understory was determined differently, by comparing L_e measured from the LAI-2000 with destructive sampling. Owing to the practical difficulty in running the tram beneath the understory canopy, no systematic sunfleck data were taken to characterize the understory architecture. Some trial measurements were made using the TRAC, but the gap size distribution approach became exceedingly difficult because radiation reaching the top of the understory was not uniform. The Ω value, taken as L_e/L, where L is the destructive LAI, was found to be 0.98, indicating that the foliage of the understory was very close to the random condition.

Fig. 14 shows the seasonal course of LAI for both the overstory and understory. Using LAI-2000 measurements taken within the vicinity of the tower, the aspen LAI was calculated as $L = ((L_e/\Omega) - a) \times 1.15$, where Ω is a function of the time of year (Fig. 13) set at a maximum of unity, a is the pre-leaf L_e measurement, with a value of 0.62, and the 1.15 represents the 15% correction owing to blue-light scattering. Aspen bud emergence began in late April, followed by leaf emergence beginning in mid-May and culminating in a maximum LAI of 2.4 by mid-July. This value is in close agreement with LAI = 2.3 obtained by leaf-litter basket collection in September over a 25 m transect also near the vicinity of the tower (J. Fuentes, personal communication, 1996). Subsequent leaf-curling and occasional branch loss resulted in a slight decrease in LAI through the remainder of the summer, until senescence began during the second week of September. Owing to the spatial heterogeneity of LAI in the transects emanating away from the tower, the seasonal course of aspen

LAI presented in Fig. 14 could be increased by the previously discussed 20% to be a more realistic estimate in the meteorological footprint of the tower. For the hazelnut understory, the seasonal LAI was calculated from LAI-2000 temporal measurements as $L = (L_e/\Omega) - a$, where Ω was set at 0.98 when the hazelnut was in full leaf (mid-June to 1 September) and was set equal to unity at all other times, and a was equal to 0.34 (determined from pre-leaf L_e measurements). The correction for blue-light scattering is incorporated in Ω, as the ratio of the L_e to the destructive LAI incorporates not only Ω, but all factors relating to any discrepancy between L_e and LAI. Similar to the aspen, hazelnut bud emergence began in late April, followed by leaf emergence in mid-May. Leaf growth ended in late June, with a maximum LAI of 3.3 being reached by mid-July. Hazelnut LAI was maintained close to the maximum until senescence began in the third week of August (2 weeks before the aspen).

5. Discussion

Plant canopy architecture and the radiation environment are closely related to each other. So far, we have examined these two aspects in various details. The results presented above can be used in different ways depending on the need.

A simple way to estimate the irradiance of the global radiation, PPFD and net radiation between the overstory and the understory is to use the L_e-based bulk extinction coefficient. It appears that the bulk extinction coefficients for these radiation variables are only weakly dependent on the solar zenith angle and can be treated as constants without incurring large errors. To improve the estimation of the radiation environment in the canopy, it is necessary to separate the direct and diffuse radiation streams. The calculation of both direct and diffuse radiation can be done based on the effective LAI, which is easily measured with many optical instruments (Black et al., 1991). If the angular distribution of leaves is spherical (random), L_e is sufficient for this purpose. Otherwise, the projection function $G(\theta)$ needs to be defined, but it is usually obtained simultaneously with L_e. Therefore, for the purpose of estimating the radiation environment with reasonable accuracies, only L_e and $G(\theta)$ are needed, and the difficulty in obtaining LAI through Ω may be avoided. However, we do not rule out the possible improvements to be made in modeling diffuse radiation using canopy architectural parameters. Our work using the multilayer model of Norman (1979) based on L_e resulted in considerable underestimation of the diffuse irradiance beneath the canopy. This may be due to the fewer forward (downward) multiple scattering events between foliage clumps than between leaves assumed in the model, suggesting that for accurate modeling, canopy architectural parameters are needed. Nevertheless, for the purpose of estimating the global irradiance, such detailed modeling for a relatively small component may not always be critical.

However, in many ecological applications, it is LAI rather than L_e (though this distinction has not been made clearly in the literature) that is needed, because LAI defines the photosynthetically active leaf surface area responsible for plant growth and CO_2 uptake (Bonan, 1993). LAI is also important for estimating rainfall interception by the foliage, especially for completely wet canopies during a storm event. For these purposes, LAI cannot be replaced by L_e, and the extra effort to obtain the clumping index is warranted.

In remote sensing applications, accurate modeling of the small reflected solar radiance from plant canopies is fundamental in retrieving the surface information. Such modeling requires not only LAI but also some canopy architectural parameters (Li and Strahler, 1992; Chen and Leblanc, 1997). Both the F and P approaches are useful for this purpose. The F approach provides good estimates of the clumping index, and the P approach can be used to derive several canopy architectural parameters such as the imaginary clump surface area and clump size. These canopy architectural parameters are the basis for canopy directional reflectance models (Roujean et al., 1992).

6. Conclusions

Synthesizing tram measurements, LAI-2000 measurements and destructive sampling, the effect of leaf area and structure on the radiation regime beneath a boreal aspen forest was determined. The following conclusions can be drawn: (1) radiation extinction on a plant-area (L_e) basis before leaf emergence was higher than after leaf emergence; (2) after leaf emergence, the ratios of below to above fluxes for S, PPFD and R_n were 0.33, 0.26 and 0.26, respectively; (3) $G(\theta)$ for the aspen was relatively constant throughout the growing season, which implies that the distribution of leaf angles was random (spherical); (4) the aspen canopy was clumped ($\Omega = 0.7–0.85$); (5) the hazelnut canopy was planophile and unclumped ($\Omega = 0.98$); (6) at leaf maturity, the LAI of the aspen and hazelnut in the vicinity of the tower was 2.4 and 3.3, respectively; (7) the average LAI of the aspen is 2.9 over the 300 m transect in the southwest direction from the tower, representing the footprint area of fluxes measured at the tower.

References

Baldocchi, D.D., Detlef, R.M., Hutchinson, B.A. and McMillen, R.T., 1984. Solar radiation within an oak–hickory forest: an evaluation of the extinction coefficient for several radiation components during fully-leafed and leafless periods. Agric. For. Meteorol., 32: 307–322.

Black, T.A., Chen, J.M., Lee, X. and Sagar, R.M., 1991. Characteristics of shortwave and longwave irradiance under a Douglas-fir forest stand. Can. J. For. Res., 21(7): 1020–1028.

Black, T.A., den Hartog, G., Neumann, H.H., Blanken, P.D., Yang, P.C., Russell, C.A., Nesic, Z., Lee, X., Chen, S.G., Staebler, R. and Novak, M.D., 1996. The annual cycles of carbon dioxide and water vapour fluxes in and above a boreal aspen forest. Global Change Biol., 2: 219–229.

Bonan, G.B., 1993. Importance of leaf area index and forest type when estimating photosynthesis in boreal forests. Remote Sens. Environ., 43: 303–314.

Chen, J.M., 1996a. Optically based methods for measuring seasonal variation of leaf area index in boreal conifer stands. Agric. For. Meteorol., 80: 135–163.

Chen, J.M., 1996b. Canopy architecture and remote sensing of the fraction of photosynthetically active radiation absorbed by boreal conifer forests. IEEE Trans. Geosci. Remote Sens., 34: 1353–1368.

Chen, J.M. and Black, T.A., 1992a. Defining leaf area index for non flat leaves. Plant Cell Environ., 15: 421–429.

Chen, J.M. and Black, T.A., 1992b. Foliage area and architecture of plant canopies from sunfleck size distributions. Agric. For. Meteorol., 60: 249–266.

Chen, J.M. and Cihlar, J., 1995a. Plant canopy gap size analysis theory for improving optical measurements of leaf area index. Appl. Opt., 34: 6211–6222.

Chen, J.M. and Cihlar, J., 1995b. Quantifying the effect of canopy architecture on optical measurements of leaf area index using two gap size analysis methods. IEEE Trans. Geosci. Remote Sens., 33: 777–787.

Chen, J.M. and Leblanc, S.G., 1997. A bidirectional reflectance model based on conifer canopy architecture. IEEE Trans. Geosci. Remote Sens., in press.

Chen, J.M., Black, T.A. and Adams, R.S., 1991. Evaluation of hemispherical photography for determining plant area index and geography of a forest stand. Agric. For. Meteorol., 56: 129–143.

Hutchinson, B.A. and Matt, D.R., 1976. Beam enrichment of diffuse radiation in a deciduous forest. Agric. Meteorol., 17: 93–110.

Kabzems, A., Kosowan, A.L. and Harris, W.C., 1986. Mixedwood section in an ecological perspective: Saskatchewan. Tech. Bull. 8, Saskatchewan Parks and Renewable Resources, Regina, Saskatchewan.

Li, X. and Strahler, A.H., 1992. Geometric-optical bidirectional reflectance modeling of the discrete crown vegetation canopy: effect of crown shape and mutual shadowing. IEEE Trans. Geosci. Remote Sens., 30: 276–291.

Miller, E.E. and Norman, J.M., 1971. A sunfleck theory for plant canopies. I. Lengths of sunlit segments along a transect. Agron. J., 63: 735–738.

Miller, J.B., 1967a. A formula for average foliage density. Aust. J. Bot., 15: 141–144.

Miller, P.C., 1967b. Leaf temperature, leaf orientation and energy exchange in quaking aspen (*Populus tremuloides*) and Gambell's oak (*Quercus gambellii*) in central Colorado. Oecol. Plant., 2: 241–270.

Miller, P.C., Stoner, W.A. and Tieszen, L.L., 1976. A model of stand photosynthesis for the wet meadow tundra at Barrow, Alaska. Ecology, 57: 411–430.

Nilson, T., 1971. A theoretical analysis of the frequency of gaps in plant stands. Agric. Meteorol., 8: 25–38.

Norman, J.M., 1979. Modeling the complete crop canopy. In: B.J. Bartifield and J.F. Gerber (Editors), Modification of the Aerial Environment of Plants. American Society of Agricultural Engineers, St. Joseph, MI, pp. 249–277.

Rauner, J.U.L., 1976. Deciduous forests. In: J.L. Monteith (Editor), Vegetation and the Atmosphere, Vol. 2, Case Studies. Academic Press, London, pp. 241–264.

Ross, J., 1981. The Radiation Regime and Architecture of Plant Stands. Junk, London, 391 pp.

Roujean, J.-L., Leroy, M. and Deschamps, P.-Y., 1992. A bidirectional reflectance model of the Earth's surface for correction of remote sensing data. J. Geophys. Res., 97: 20455–20468.

Running, S.W. and Coughlan, J.C., 1988. A general model of forest ecosystem processes for regional applications. I. Hydrologic balance, canopy gas exchange and primary production processes. Ecol. Model., 42: 125–154.

Sellers, P.J., Mintz, Y., Sud, Y.C. and Dalcher, A., 1986. A simple biosphere model (SiB) for use within general circulation models. J. Atmos. Sci., 43: 505–531.

Stoner, W.A., Miller, P.C. and Miller, P.M., 1978. A test of a model of irradiance within vegetation canopies at northern latitudes. Arct. Alpine Res., 10: 761–767.